ARTICLES

A Frozen Tube Model of Melting Point Depression of Solvents in Entangled Polymer Systems

Yoshio Hoei*

S & S Japan Company, Ltd., 6-1-18, Hamazoe-dori, Nagata-ku, Kobe, Hyogo 653-0024, Japan

Yoshiyuki Ikeda and Muneo Sasaki

Faculty of Science and Technology, Konan University, 8-9-1, Okamoto, Higashinada-ku, Kobe 658, Japan

Received: March 20, 2002; In Final Form: October 17, 2002

The entanglement model, which was proposed previously on the melting point depression of a crystalline low molecular weight diluent in an un-cross-linked amorphous polymer, was modified so as to be consistent with a frozen tube model. In the latter model, the crystallization of the diluent occurs within the entangled polymer chains, which act as a confining frozen and hard tube involving an unfrozen solvent within. The new model accounts reasonably for the experimental observations and provides estimates of the diluent crystal size, frozen tube size, and other well-defined parameters for the un-cross-linked systems. The calculation based on the new model for two different cases of lightly cross-linked and un-cross-linked rubber mixtures can explain well the crystal sizes determined by X-ray and NMR measurements for some relevant concentrations.

Introduction

The purpose of this paper is to attempt to analyze, with a simple model, a melting point depression (mpd) that has been observed for small molecules in an un-cross-linked amorphous polymer.[1−7] This attempt will be physicochemically and industrially important because it will provide more detailed molecular information on such binary materials from the viewpoints of molecular science. In this work, the prior model[8] will be revised and tested on the basis of the experimental mpd data for two kinds of systems on lightly chemically cross-linked natural rubber (NR)−benzene and un-cross-linked poly(isoprene) (IR)−*n*-docosane mixtures. Particularly, we will examine how the diluent crystal size changes with the observed mpd and so with the concentrations in the mixtures. And results predicted from the revised model will be compared with those determined experimentally by X-ray and nuclear magnetic resonance (NMR). How the revised model has been developed is described below.

The classical expression for the mpd of a single-crystal particle of size (ζ_0) is given by the Gibbs−Thomson (GT) equation,[6,8−11]

$$(1/T_m - 1/T_m^\circ)(h_0/R) = q\sigma_0/(\zeta_0 R T_m) \quad (1)$$

where T_m is the solvent melting temperature in the mixture, T_m° is the melting temperature of the pure solvent, h_0 is the heat of fusion of the pure solvent, R is the gas constant, σ_0 is the interfacial energy of the crystal particle, and q is the shape factor (e.g., $q = 2$ for cylindrical crystals and $q = 4$ for cubic or spherical crystals). But, the GT model does not consider any effects induced by mixing between solvent and polymer for the case of binary mixtures. On the other hand, the presence of unfrozen solvent molecules in frozen polymer mixtures has been experimentally verified by different workers,[6,11,12] and in the case of the frozen NR−benzene mixtures, unfrozen benzene molecules surrounding the polymer chains were observed at lower temperatures than T_m° using both NMR and differential scanning calorimetry (DSC) measurements.[6] The presence of the local solution phase is consistent with a melting model of solvent crystallites in a polymer solution, as proposed by Hoei, Yamaura, and Matsuzawa[13] and by Hoei, Ikeda, and Sasaki.[8] The previous work[8] considering the mixing entropy and polymer−solvent interaction energy[8,13] derived the combined form of the Flory−Huggins (FH)[1,14] and GT equations (abbreviated to to FH-GT equation) for the solvent crystal particles in the solution phase:

$$(1/T_m - 1/T_m^\circ)(h_0/R) = \ln(1 - \phi) + \phi + \chi\phi^2 + 4\sigma_0/\zeta_0 R T_m \quad (2)$$

where ϕ is the volume fraction of polymer and χ is the FH polymer−solvent interaction parameter. Equation 2 stands for a thermodynamically reversible and equilibrium relation that the chemical potential of the solvent crystal phase equals to that of the solution phase at the melting point. By using eq 2 for the mpd data observed by Jackson and McKenna,[6] we attempted to predict crystal sizes for a series of lightly cross-linked NR−benzene mixtures at different concentrations.[8] The mixtures could be taken to be virtually indistinguishable from an un-cross-linked rubber that can fit a Flory−Huggins[1,2] curve. The predicted crystal size values were much larger than those determined from eq 1, and we modified the above FH-GT model

10.1021/jp020772c CCC: $25.00
Published on Web 01/28/2003

to an entanglement model[8] by extending simply the conventional Frenkel−Flory−Rehner (FR) swelling theory.[14,15] This model is based on the notion that physically entangled end-to-end points should behave elastically like chemical cross-links in a swollen mixture with a good solvent because each individual chain expands in the mixture. There could be an extra contribution to the elastic free energy induced by entanglements, and that entangled chains dissipate as the polymer is diluted. This might become an important factor to affect the mpd of the physical network. Therefore another revised equation (abbreviated to FH−GT−FR equation) for the physical networks was proposed as[8]

$$(1/T_m - 1/T_m^\circ)(h_0/R) = \ln(1-\phi) + \phi + \chi(\phi,T_m) + dV_0[1/M_c + P_e/M_e(\phi)](\phi^{1/3} - \phi/2) + 4_0/\zeta_0 RT_m \quad (3)$$

and

$$M_e(\phi) = M_e^*/\phi^{j-1} \qquad 2.1 < j < 2.3 \quad (4)$$

where $M_e(\phi)$ is the entanglement molecular weight at concentration ϕ, M_e^* is the bulk entanglement molecular weight defined by the average molecular weight between entanglements, P_e is in the range $0 \le P_e \le 1$ and is the probability that an entanglement is trapped, d is the density of polymer at T_m, V_0 is the molar volume of the solvent, and M_c is the molecular weight between chemical cross-links. Equation 4 is Graessley's empirical relationship,[16a] which shows with eq 3 together that the entanglement density varies, depending on the solvent concentration. Also, $1/M_c$ in eq 3 can be omitted if $M_c \gg M_e(\phi)$.

Again, we estimated benzene crystal sizes for the weakly cross-linked NR mixtures of Jackson−McKenna[6] by use of eq 3,[8] and the calculated sizes resulted in fairly good agreement with the previous X-ray observations[10] but still larger than those from eq 1 or the Flory coil sizes (see eq 10). Equation 3 also showed more improvement than eq 2 in estimation of crystal size at the same concentration. The result implied that there could be a concentration dependence of benzene crystal size. In fact, this will be much more clearly seen in the case of IR−docosane, as reported later. The concentration dependence of the mpd ($\Delta T = T_m^\circ - T_m$) would be connected with a change in the entangled end-to-end distance with concentration; that is, the entangled polymer chains could divide the crystal structure into their mesh size that is smaller as the polymer concentration is larger so that the heat of fusion would be lowered, resulting in the lowered mpd.

To get quantitatively satisfactory results, this work will introduce two effects to the above FH−GT−FR relation. One is that entangled chains that form a physical network would be deformed (or extended) to a fairly large extent during solvent crystallization. Another is the presence of unfrozen solvent molecules that locally plasticize polymer chains, as already stated.[6,11,12,17] In this connection, if a system is at solid−liquid equilibrium, an extra elastic free energy contribution in the frozen state should be added to that in the swelling state prior to freezing. In the present theory presented here, therefore, we will apply a "frozen" tube concept to formulate a spatial confinement of the "plasticized" networks linked by unfrozen solvent domains, as illustrated in Figure 1.

Frozen Tube Model

The revised model is based on the thought that the tube concept of chain confinement provides a basis for estimating an additional size scale. In particular, in addition to the chemical potential of "unfrozen-and-swollen" systems that arises from the swelling deformation term there will be also an elastic term characterized by a tube wall that results from the average repulsive force exerted by the surrounding chains, as seen in Figure 1.[18] The structural parameters related to the tube diameter and crystallographic cross-sectional areas (or van der Waals-like thickness per polymer chain) have also been estimated for many bulk polymers.[19−22] In the case of melting of a solvent in a frozen-and-swollen equilibrium state, the tube diameters should correspond to the crystallite dimension.

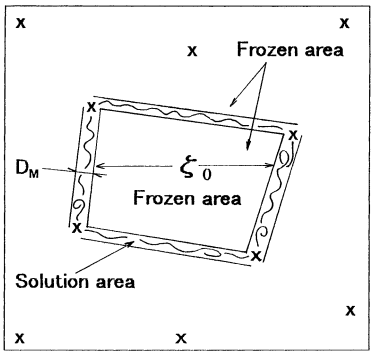

Figure 1. Schematic representation of frozen hard tubes having an unfrozen solvent and a chain within. The symbol (×) indicates an entanglement coupling point.

As already stated, considering the presence of unfrozen solvent molecules in frozen polymer mixtures,[6,11,12] it may be thought that the swollen chains that are associated with the unfrozen solvent would be separated from the crystalline solvent. Further, they can be considered as confined between the frozen solvent walls. Hence in the thermodynamic expressions that describe melting, it is important to consider the extra elastic energy caused by this confinement. We model this as a tube containing unfrozen solvent molecules that plasticize locally the polymer chains. Thus, the tube is not the same as that corresponding to the "unfrozen-and-swollen" state tube. To introduce an extra frozen-state term to eq 3 and to give its relation to physical networks that are highly entangled physically or lightly cross-linked chemically, we employ a Daoud−de Gennes' treatment[18,23] that considers only a change in the dimension of a single real (not ideal) chain in a good solvent. In the present case the tube wall consists of frozen solvent. Further, that single tube model may be used for the frozen network in a manner similar to the FR swelling procedure. Namely, we assume the elastic change in a network tube occurs affinely. Daoud and de Gennes deduced a scaling relation $L/na \cong (a/D)^{2/3}$ between the end-to-end distance L (corresponding to the tube length) of the single chain and the tube diameter D, where n is the number of segments in the tube and a is the segment length. Then for the case of the crystallized solvent a term corresponding to the $1/M_e$ swelling term in eq 3 is represented as

$$1/M \cong (1/m)(a/L)(a/D)^{2/3} \quad (5)$$

where m is the molecular weight of the segment. When this term is added to eq 3 as an FR-type term, a new equation for the mpd is obtained, which involves the "freezing" parameters of the tube length and the diameter. Two considerations are essential in writing the final mpd equation: (1) if the systems are in an ideal and frozen equilibrium, the tube length is equal to the crystal length, viz., $L = \zeta_0$, and, (2) in order that the insides of the network tubes remain unfrozen, the inner concentration ϕ_t must be higher than the overall concentration

TABLE 1: Estimated Values of Crystal Size for Benzene in M_c = 21 800 NR, According to the Previous and Revised Models

					FH-GT-FR (eq 3)		eq 6		coil size[g]
ø[a]	T_m[a] (°C)	ΔT[b] (°C)	χ_M[c]	$M_e(ø)$[d] $j = 2.1$	ζ_0 (nm) $P_e = 0$	ζ_0 (nm) $P_e = 1$	ζ_0 (nm) $\omega_0 = 1$[e]	ζ_{cr} (nm) $\omega_0 = 0$[f]	R_F (nm) $j = 2.1-2.3$
0.134	5.00	(0.2)	0.400	(21800)	(1175.7)	(1175.7)	499	448	(11.5)
0.381	4.43	1.1	0.403	10116	negative	negative			
0.396	0.82	4.7	0.406	9696	80.1	69.8	53	50	7.1−7.9
0.437	1.25	4.2	0.406	8700	282.6	178.8	128	121	6.6−7.3
0.519	−1.73	7.2	0.410	7201	175.2	122.2	88	84	5.9−6.4
0.543	−3.01	8.5	0.412	6852	132.2	98.5	71	68	5.7−6.2
0.562	−5.99	11.5	0.416	6597	46.4	41.3	31	30	5.6−6.0
0.572	−6.20	11.7	0.416	6470	50.8	44.6	33	32	5.5−5.9
0.647	− 10.24	15.7	0.424	5650	60.2	50.9	37	36	5.1−5.4
0.722	− 15.77	21.3	0.437	5008	96.3	72.9	52	51	4.8−4.9

[a] Data extracted from $\Delta T-ø$ plot by Jackson and McKenna.[6] [b] Calculated from $\Delta T = T_m° - T_m$ and $T_m° = 5.5$ °C (the melting point of pure benzene crystal). [c] Calculated from the temperature−composition dependent relationship established by Maron et al.[8,27] [d] Calculated from eq 3 taking $j = 2.1$ and $M_e = 3500$.[16a,c] [e] Calculated for the extreme condition ($ø_t = \phi$, $\omega_0 = 1$) using eqs 6−8. [f] Calculated for the crystal condition ($ø_t = 1, \omega_0 = 0$) using eqs 6−8. [g] Calculated for $m = 136$, $a = 0.81$ nm (as two isoprene units), $\chi = 0.43$, and $M_e(ø)$ values for $j = 2.1$ and 2.3 (see eq 3), using eq 10.

ϕ ($\phi_t > \phi$). Hence, eq 3 for frozen physical networks becomes

$$(1/T_m - 1/T_m°)(h_0/R) = \ln(1-ø) + ø + \chi(\phi,T_m) + dV_0[1/M_e(ø) + (1/m)(a/\zeta_0)\{a/D_M(ø)\}^{2/3}](ø^{1/3} - ø/2) + 4_0/\zeta_0 RT_m \quad (6)$$

In eq 6 $D_M(\phi)$ is the tube diameter at melting equilibrium, which is generally expressed by a function of concentration, and $P_e = 1$ for the entanglement term on the assumption that the networks consist of elastically effective entanglements alone.

As already described, the $1/M_e$ term in eq 6 means that the elastic free energy contribution decreases so that the mpd becomes small as the polymer is diluted. Obviously this term is different from the $1/M_c$ term for a swollen network, which is given from the elastic free energy stored in the network and independent from concentration. The frozen $1/D_M(\phi)$ term, which expresses that the chain mobility is confined within the frozen tube, is newly added to the $1/M_e$ term (i.e., the entanglement dissipation term) in eq 6, and such a chain confinement effect becomes smaller as the polymer is diluted as well as the entanglement dissipation effect.

Furthermore, when one analyzes experimental mpd data using eq 6, the inner volume fraction ϕ_t and the degree of crystallinity ω_0, which will be mentioned below, are useful. The former is defined as the volume fraction of a single chain inside a tube of diameter D_M and length ζ_0 and given by

$$ø_t = Sa[M_e(ø)/m]/[\zeta_0 \pi D_M(ø)^2/4] \quad (7)$$

In eq 7 S is the crystallographic cross-sectional area of the chain. Although Daoud and de Gennes proposed another relation $\phi_t \sim (a/d)^{4/3}$ by a scaling treatment for the single chain confinement,[18,23] we will use eq 7 because the numerical coefficient (prefactor) in the relation of ϕ_t is unknown. ω_0 is defined by the ratio of the amount of frozen solvent to the total amount of solvent in a physical network system as given by

$$\omega_0 = (1/ø_t - 1)/(1/ø - 1) \quad (8)$$

where $\phi_t > \phi$, $0 < \omega_0 < 1$. For a completely crystallized system, $\omega_0 = 1$ and $\phi_t = \phi$, however, the tube volume V_t ($=\zeta_0 \pi D_M^2/4$) is at maximum. Hence, when any direct experimental data of ω_0 are absent, the limiting condition of $\omega_0 = 1$ becomes a useful reference point in the evaluation of D_M and ζ_0, which provide an estimate of the maximum size of the tube. At the same time, the limit of no freezing of the tube implies that $\omega_0 = 0$, $\phi_t = 1$ and the tube volume takes the minimum value equal to the crystallographic volume of the polymer chain $V_{tcr} = Sa(M_e/m)$ inside the tube. As stated below, we will mainly compare crystal sizes estimated on the above two extreme conditions with experimental results.

Results and Discussion

NR−Benzene Mixtures. Jackson and McKenna[6] gave a concentration dependence of mpd on the lightly chemically cross-linked NR−benzene mixtures of M_c = 21 800. On the basis of those data, the previous report[8] estimated benzene crystal sizes using eqs 2 and 3. It was concluded that eq 3 was better in fitting observed sizes to theoretically calculated coil sizes. In this section, we apply the revised model (eqs 6−8) based on the tube concept to the mpd data of Jackson and McKenna[6] and demonstrate that the model is more improved than the previous one (eq 3). Here, a bulk entanglement molecular weight, $M_e^* = 3500$ (at −30°C), is the same as that used in the prior works.[8,16c]

Equation 6 involves the tube parameter D_M at freezing equilibrium. However, insofar as we know, there are no available data for the benzene−NR mixtures. If ω_0 for frozen mixtures with a solvent are independently measured, V_t can be evaluated from eqs 7 and 8 using the known crystallographic polymer thickness S (and V_{cr}) from the literature.[19,20−22] Accordingly, if either D_M or ζ_0 is experimentally available, the parameter values become determined. At this time, no such complete data set for the benzene−NR mixtures exists. However, for the completely crystallized systems (i.e., $\omega_0 = 1$), calculations based on eqs 6−8 can be carried out.

Tables 1 and 2 show the values of ζ_0 and D_M for $\omega_0 = 1$. Also given are $\zeta_{0,cr}$ and D_{cr} and values for $\omega_0 = 0$. Other related parameter values, V_t (for $\omega_0 = 1$), $V_{t,cr}$ (for $\omega_0 = 0$), and the number of unfrozen benzene molecules per tube N_{ot} (for $\omega_0 = 1$), are shown in Table 2. These values were calculated by assuming the following basic parameter values: a crystallographic cross-sectional area is taken as $S \approx 0.28$ nm^2 determined from the unit cell parameters of IR crystal,[20] a molecular weight per segment as $m = 136$ for two isoprene monomers, and the segment length as $a \approx 0.81$ nm. N_{ot} is determined by the relation

$$N_{ot} = V_t(1 - ø_t)/\upsilon_m \quad (9)$$

where υ_m is an approximate volume of a liquid solvent molecule. In the present case, υ_m is 0.15 nm^3 for a liquid benzene molecule.[24−26] In addition, the choice of the above segment

TABLE 2: Estimated Values of Frozen Tube Parameters for Benzene in $M_c = 21\,800$ NR, According to Equation 6

ø	D_M (nm) $\omega_0 = 1^a$	D_{cr} (nm) $\omega_0 = 0^b$	V_t (nm^3) $\omega_0 = 1^a$	V_{tcr} (nm^3) $\omega_0 = 0^b$	N_{0t} $\omega_0 = 1^a$
0.134	0.8	0.3	271	36	1567
0.381					
0.396	1.0	0.6	41	16	164
0.437	0.6	0.4	33	14	125
0.519	0.6	0.4	23	12	74
0.543	0.6	0.4	21	11	64
0.562	0.9	0.7	19	11	56
0.572	0.9	0.6	19	11	54
0.647	0.7	0.6	14	9	34
0.722	0.5	0.4	11	8	21

[a] Calculated for the extreme condition ($ø_t = \phi, \omega_0 = 1$) using eqs 6−8. [b] Calculated for the crystal condition ($ø_t = 1, \omega_0 = 0$) using eqs 6−8.

length is thought to be appropriate when compared with the diameter of the spherical benzene molecule.

We also show the previous results (for $P_e = 0$ and 1)[8] in Table 1, calculated using eq 3. Of necessary parameters appearing in eqs 3 and 6, the interaction parameter χ is of a temperature−concentration dependent type (χ_M).[8,27] The other important values are $h_0(T_m°) = 9.96$ kJ/mol (where $T_m° = 5.5$ °C) and $\sigma_0 = 1.57 \times 10^{-6}$ J/cm^2.[6,24] Further details should be referred to the literature.[8] In Table 1, we also show the range of Flory's coil size (R_F) for the mixtures at different ϕ, which signifies the spatial chain expansion in benzene. The limiting values of R_F are calculated for the values of $M_e(\phi)$ by setting $j = 2.1$ and 2.3 in eq 4, according to the following relation for a polymer chain in a good solvent[18]

$$R_F \cong a(1 - 2\chi)^{0.2} n^{0.6} \tag{10}$$

where n is the number of segments composing the chain so that $n = M_e(\phi)/m$ in the case of an entanglement network chain of $M_e(\phi)$. In Tables 1 and 2, it is seen that a maximum value of D_M for $\omega_0 = 1$ is only slightly larger than the minimum value of D_{cr} for $\omega_0 = 0$, and also ζ_0's for $\omega_0 = 0$ and 1 are almost the same for both cases. What we emphasize here is that if the ζ_0 values estimated using eq 6 are compared with the previous results, the ζ_0 values should be nearer to the corresponding entanglement spacings R_F.

On the other hand, if the ζ_0 and ϕ values determined by X-ray measurement[10] of $\zeta_0 = 64$ nm at $\phi = 0.34$ for the chemically un-cross-linked system and $\zeta_0 = 57$ nm at $\phi = 0.24$ for the lightly chemically cross-linked case, the calculated crystal sizes based on the revised model, rather than the prior model, are in better agreement with the measured ones. Considering that a similar trend is found in the case of IR−docosane mixtures, as described later, the above X-ray data appear to be fairly accurate. Further, although the estimated tube parameter values in Table 2 are not greatly different from those in the case of $\phi_t = \phi$, an essential condition for mpd to occur, i.e., $\phi_t > \phi$, is reasonably satisfied. Obviously these parameters predict also that the tube is a long capillary, which agrees with the observed morphological result by Karnig and Karge.[17] It is worth noting that, in the frozen state, a change in ω_0 might be very sensitive to even a slight change in the number of unfrozen solvent molecules N_{ot} in a tube.

In final, we comment on a variability in crystal size due to a change in the index value (j) appearing in eq 4 and due to the temperature dependence of the heat of fusion of benzene (h_0) in bulk phase. Actually, the j value between $j = 2.1$ and 2.3 had little affect on crystal size as well as on the corresponding R_F, as seen in Table 1. In deriving eq 3 or 6, h_0 is assumed to be temperature independent near the melting point of the pure solvent ($T_m°$).[8,13] When we consider the temperature dependence in general, h_0 at temperature T can be estimated by using the general thermodynamic relation $h_0(T) = h_0(T_m°) - (T_m° - T)\Delta C_p$ where ΔC_p ($=C_p(T_m°) - C_p(T)$) stands for the difference in heat capacity between the liquid state and the solid state. In the case of benzene, C_p values can be determined by interpolating the experimentally linear relationship[28] of $C_p(T)$ against T between a given molten-state temperature (higher than $T_m° = 5.5$ °C) and approximately −73 °C. We recalculated ζ_0 and ζ_{0cr} using the C_p values thus determined. Consequently, the value of h_0 for the lowest melting point was slightly approximately 2.5% below $h_0(T_m°)$, and then there was no significant difference between ζ_0 and ζ_{0cr}, as found in Table 1.

IR−*n*-Docosane Mixtures. *Comparison with Prior Model.* We will further demonstrate that the proposed model seems to be more consistent than the previous model[8] in an IR−*n*-docosane system as well as the above NR−benzene system. An experimental data set of mpd for this system was previously reported by Ikeda and Hoei,[7] which was obtained using an IR of the number average molecular weight $M_n \approx 800\,000$.[29] Such molecular weight will be large enough for the chain molecules to entangle each other because its bulk entanglement molecular weight was estimated to be $M_e* = 3120-5100$ at 25 °C.[16a,16b,19] In Table 3 we show the previous results for the mixture samples at different ϕ, in which the equilibrium melting points (peak values) T_m were determined by extrapolating to zero heating rate in the DSC measurement.[7] At the same time, they obtained $h_o(T_m°) = 77.5$ kJ/mol ($C_{22}H_{46}$) and $T_m° = 44.7$ °C for the pure docosane used in the experiment, and the T_m vs ϕ curve fitted best to a Flory−Huggins curve for $\chi \approx 0.30$ with h_0 and $T_m°$ values.[7]

Table 3 shows a set of crystal parameter values of ζ_0, D_M, V_t, and N_t calculated from our revised model (i.e., eqs 6−8) directly using the above mpd data.[7] In calculating the crystal parameters, one needs to know not only the three observed parameter values (h_o, $T_m°$, and χ), but several others, i.e., σ_0 and d_o (or V_0) for the pure *n*-docosane, and S and M_e* for IR. As for σ_0, Turnbull and Cormia obtained $\sigma_0 = 9.64 \times 10^{-7}$ and 8.2×10^{-7} J/cm^2 for *n*-octadecane ($C_{18}H_{38}$) and *n*-tetracosane ($C_{24}H_{50}$), respectively, by the kinetic experiment of nucleation in small droplets.[30] But, because we know no available data on *n*-docosane, we simply take the nearly middle value for *n*-octadecane and *n*-tetracosane to be $\sigma_0 = 9 \times 10^{-7}$ J/cm^2. The density is taken to be $d_o = 0.779$ g/cm^3 at the melting point of 44.1 °C,[31] which was adopted when Sayer, Patterson, and Keays experimentally obtained density vs temperature relationships for a series of *n*-alkanes including *n*-docosane.[31] In fact, this melting point is slightly different from 44.7 °C by Ikeda and Hoei,[7] and also there is $d_o = 0.777$ g/cm^3 at 44.4 °C found from the literature.[32] It may be attributed to difference in purity, crystalline state, or experimental method or difficulties in measuring density at the melting point. Nevertheless, we combine the density by Sayer et al.[31] with the melting point by Ikeda and Hoei[7] because the present work is based on the mpd data of Ikeda and Hoei. It will be found later that using a fixed value of *n*-docosane density $d_o(T_m°)$ in eq 6 is not a serious problem despite the fact that it should be generally a function of temperature. Also, we take as $S \approx 0.28$ nm^2 for IR, the same as the NR−benzene system.

Now, we can evaluate all crystal parameters by using the above characteristic values in eqs 6−8. This evaluation is also shown in Table 3, in which are shown two limiting cases, ω_0

TABLE 3: Estimated Values of Frozen Tube Parameters for Docosane in IR, According to the Revised Model

ø	T_m (°C) $[\Delta T]^a$	$M_e(ø)^b$ $[R_F$ (nm)$]^c$	ζ_0 (nm) $\omega_0 = 1^d$	ζ_{0cr} (nm) $\omega_0 = 0^e$	D_M (nm) $\omega_0 = 1^d$	D_{cr} (nm) $\omega_0 = 0^e$	V_t (nm^3) $\omega_0 = 1^d$	V_{tcr} (nm^3) $\omega_0 = 0^e$	N_{0t} $\omega_0 = 1^e$
0.210	44.5	17366	285	243	0.78	0.39	138	29	50
	[0.19]	[12−20]	209	140	0.92	0.51	138	29	50
			$\hat{A} = 247$	383	$\hat{A} = 0.85$	0.45	$\hat{A}$ =138	29	$\hat{A} = 50$
0.300	44.2	11730	152	133	0.74	0.43	65	19	21
	[0.45]	[10−16]	107	77	0.88	0.57	65	19	21
			$\hat{A} = 129$	105	$\hat{A} = 0.81$	0.50	$\hat{A} = 65$	19	$\hat{A} = 21$
0.480	43.4	6995	100	91	0.55	0.40	24	12	6
	[1.25]	[7−12]	63	50	0.70	0.54	24	11	6
			$\hat{A} = 81$	70	$\hat{A} = 0.62$	0.47	$\hat{A} = 24$	11	$\hat{A} = 6$
0.510	43.2	6543	93	85	0.54	0.40	21	11	5
	[1.48]	[7−11]	58	46	0.68	0.55	21	11	5
			$\hat{A} = 75$	65	$\hat{A} = 0.61$	0.47	$\hat{A} = 21$	11	$\hat{A} = 5$
0.570	42.6	5790	78	72	0.52	0.41	12	8	2
	[2.07]	[6−10]	48	40	0.67	0.55	17	9	3
			$\hat{A} = 63$	56	$\hat{A} = 0.59$	0.48	$\hat{A} = 14$	8	$\hat{A} = 2$
0.680	41.1	4768	72	68	0.45	0.38	12	8	2
	[3.56]	[6−9]	42	36	0.59	0.52	12	8	2
			$\hat{A} = 57$	52	$\hat{A} = 0.52$	0.45	$\hat{A} = 12$	8	$\hat{A} = 2$

[a] $T_m° = 44.7$ °C. [b] Range calculated for $j = 2.1$ and $M_e* = 3120$ using eq 3.[16a,b,19] [c] Calculated for $m = 136$ and 476, $a = 0.81$ and 2.83 nm as two and seven isoprene units, respectively, and $\chi = 0.30$, using eq 10.[18] [d] Calculated for the extreme condition ($ø_t = \phi$, $\omega_0 = 1$) using eqs 6−8. The upper and lower values are estimated for $a = 0.81$ and 2.83 nm, respectively, and $\hat{A}$ is an average value of the two values. [e] Calculated for the crystal condition ($ø_t = 1$, $\omega_0 = 0$) using eqs 6−8. The significances of the three values are the same as above.

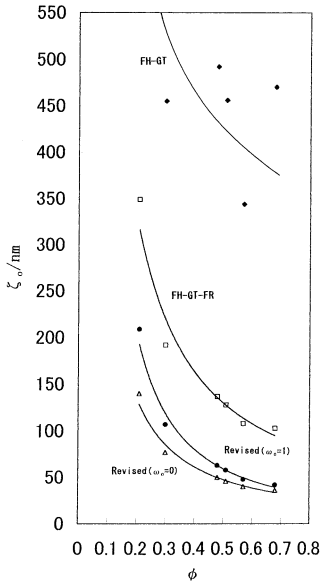

Figure 2. Plots of ζ_0 (nm) against ϕ for un-cross-linked IR−*n*-docosane mixtures, where best-fitting curves are depicted for the mpd data of Table 3 using eq 2 (FH-GT) and eq 3 (FH-GT-FR; $P_e = 1$), and for $\omega_0 = 0$ and 1 in the same way using the revised eq 6.

$= 1$ and 0, for some mixtures at concentration. Also shown are $M_e(\phi)$ values calculated for the individual mixtures using eqs 4 (being taken as $j = 1.2$ and $M_e* = 3120$) and R_F ranges estimated using eq 10. For each mixture of ϕ in Table 3, three numerical values are written for each of its crystal parameters. The values in the upper and the middle rows are calculated for $a = 0.81$ and 2.83 nm, respectively, and the value in bottom one is their mean value ($\hat{A}$). These a values mean possible segment lengths of two and seven isoprene monomer units, and $a \approx 2.68$ nm is approximately equal to the fully extended length of *n*-docosane molecule.

To compare the estimates of ζ_0 from the revised eq 6 together with eqs 7 and 8 to those from the previous equations (eqs 2−4),[8] we show plots of ζ_0 vs ϕ in Figure 2, in which the FH-GT (eq 2) and FH-GT-FR (eq 3) curves are plotted using the same data sets of ζ_0 and ϕ as in the lierature,[8] and the revised curves for $\omega_0 = 1$ and 0 are plotted using the ζ_0 values (indicated by underlines in Table 3), which is further calculated using $M_e* = 3120$ and $a = 2.83$ nm in the mpd data. What we emphasize in this section is that (1) the magnitudes of crystal sizes estimated by eq 6 approach much better than those estimated by eqs 2 and 3 to those of the corresponding R_F range in Table 3, and (2) the revised model can show a clear ϕ dependence on ζ_0. This implies that the mpd phenomenon seems to be largely influenced by elasticity induced by both chain swelling before freezing and chain confinement created by the frozen solvent.

Crystal Parameters from X-ray and NMR. Although the above results for the IR−*n*-docosane system seem consistent with the revised model as well as the NR−benzene system, we provide here additional supportive information from new observations measured on un-cross-linked IR−*n*-docosane mixtures by Ikeda and Sasaki. They determined the crystal size (ζ_0) and the amount of crystallized docosane (ω_0) for a range of concentrations in the mixtures using both small-angle X-ray scattering and broad-line NMR measurements, respectively. Although we set up no full Experimental Section in this work, as will be reported elsewhere, only a few important points are described particularly on the X-ray experiments performed by the workers: one is that they applied the well-known Guinier−Fankuchen method[33] to determine a value of crystal size in a heterogeneous crystalline system. This is because such an un-cross-linked mixture has a broad size distribution. In preparing the mixtures, *n*-docosane of over 99% purity (supplied by Nippon Seiro Co., Ltd.) was used. However, the existing small impurities in the mixtures might have underestimated the observed mean size of a crystal particle in the mixtures. Therefore, the pure IR used as the base polymer (of the number average molecular weight $M_n \approx 800\,000$)[29] to prepare the mixtures was also measured by X-ray. The X-ray diffraction intensity of the pure IR was much weaker than those of the mixtures so that there may be no adverse effects from foreign matter or crystallites that the IR material contains.

Table 4 shows the ζ_0 values determined by X-ray experiment (abbreviated to "X-ray size") for four mixtures covering the wide range of ϕ. The X-ray crystal sizes stand for a mean value due

TABLE 4: Experimentally Observed Data of ζ_0 and ω_0 and Estimated Values of Frozen Tube Parameters for Docosane in IR, According to Revised Model

	X-ray (at RT)	NMR (at 30 °C)					
ø	ζ_0 (nm)[a]	ω_0[b]	$ø_t$[c]	ζ_0 (nm)[c]	D_M (nm)[c]	V_t (nm^3)[c]	N_{0t}[c]
0.210	83−130	0.562	0.32	260	0.66	90	28
				166	0.83	90	28
				$\hat{A}$ = 213	$\hat{A}$ = 0.71	$\hat{A}$ = 90	$\hat{A}$ = 28
0.480	68−108	0.340	0.73	96	0.46	16	2
				56	0.60	16	2
				$\hat{A}$ = 76	$\hat{A}$ = 0.53	$\hat{A}$ = 16	$\hat{A}$ = 2
0.510	56−88						
0.680	49−75						
0.790		0.150	0.96	55	0.37	7	0.1
				38	0.48	7	0.1
				$\hat{A}$ = 46	$\hat{A}$ = 0.42	$\hat{A}$ = 7	$\hat{A}$ = 0.1

[a] Determined from Guinier plot, according to the Fankuchen method.[33] [b] Determined by the broad-line NMR. [c] Estimated from the NMR data ofω_0 and the mpddata in Table 3, using eqs 6−8. The upper and lower values are estimated for a=0.81 and 2.83 nm, respectively, and $\hat{A}$ is an average value of the two values.

to the distribution that each mixture has. Thus the X-ray crystal sizes can be compared with ζ_0 estimated by eq 6. In addition, we show both uncorrected and corrected mean size values for the mixtures at different volume fractions, which correspond to smaller and larger numerical values in Table 4, respectively. It was found from X-ray experiment that in $\phi = 0.21$ mixture there existed approximately 40% (by mass) of 8.9 nm sized particle, 8% 34 nm, 14% of 76 nm, and 38% of 170 nm. Of these, the smallest size (approximately 8.9 nm) is even smaller than the corresponding coil size range $R_F \approx 12-20$ nm for a = 0.81−2.83 nm, as seen in Table 3. Also, the smallest particle sizes observed in the other mixtures were almost equivalent to the corresponding R_F ranges in the table (though not shown here). Thus we simply assumed that the smallest particles detected in the $\phi = 0.21$ mixture should be only impure material, and so we obtained the mean size values shown in Table 4 by excluding the smallest particle percentage content.

In Table 4, we estimated three ϕ_t values from the corresponding NMR data of ω_0 (i.e., 0.562, 0.340, and 0.150) using eq 8. In the same table, we show also the values of ϕ_t, ζ_0, D_M, V_t, and N_{0t} for the same mixtures, estimated from both the NMR data of ω_0 and the mpd data set of Ikeda and Hoei[7] using eq 6. The results from NMR observation are compared with those seen in Table 3 in the following section.

Comparison with the X-ray and NMR Observations. Figure 3 shows plots of ζ_0 vs ϕ for $\omega_0 = 1$ and 0 from the data in Tables 3 and 4. In Figure 3, except the $\phi = 0.21$ mixture three X-ray sizes are well within the predicted ranges (for $\omega_0 = 1$ and 0) for the corresponding ϕ mixtures. For $\phi = 0.21$, the size determined by X-ray deviates largely from the predicted one; however, the experimental size by NMR agrees nearly with the predicted one.

A value of $\hat{A}$ is an approximately average value of ζ_0 calculated for $a = 0.81$ (corresponding to two isoprene units) and 2.83 nm (corresponding to seven isoprene units and approximately equal to the extended length of docosane molecule). This implies that the segment length of about 4−5 isoprene units might be required for segmental motion in the unfrozen area of IR−docosane inside the frozen tube. On the other hand, it is well-known that a long chained *n*-alkane molecule makes a folded structure at some critical chain length with hundreds of carbons.[34] Thus *n*-docosane molecules in the frozen area of the present systems will be crystallized in the extended chain state.

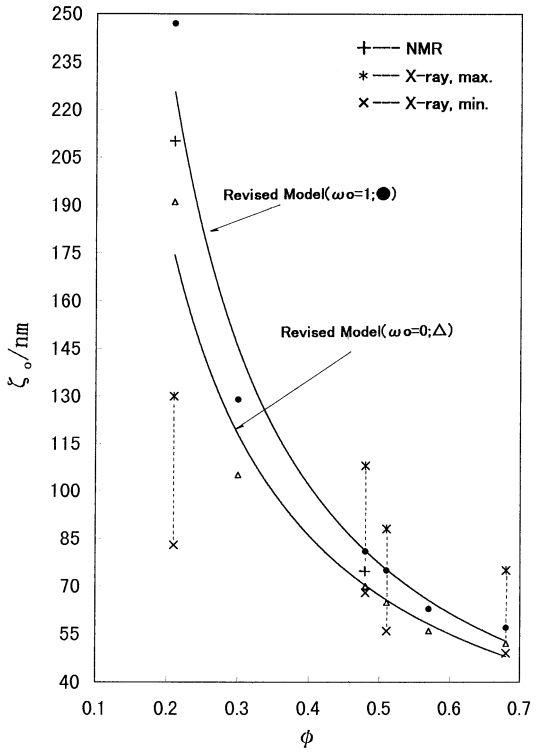

Figure 3. Plots of ζ_0 (nm) against ϕ for un-cross-linked IR−*n*-docosane mixtures, where best-fitting curves (solid lines) are depicted for the mpd data of Table 3 using the revised eq 6, and the data points from NMR and X-ray, indicated by the symbols +, *, and ×, respectively, are shown with the curves.

Although eq 6 can explain successfully the X-ray data, the ω_0 values determined by NMR experiment (abbreviated to "NMR value") would further support the effectiveness of eq 6. When we consider either case of $a = 0.81$ or 2.83 nm, the NMR values of size for $\phi = 0.21$ and 0.48 in Table 4 are within the corresponding range between ζ_{0cr} (for $\omega_0 = 0$) and ζ_0 (for $\omega_0 = 1$) in Table 3. This is clearly seen in Figure 3 where the data points for $\phi = 0.21$ and 0.48 are indicated by the symbol (+). In addition, the NMR sizes determined at $\phi = 0.79$ for a = 0.81 and 2.83 nm and the mean value ($\hat{A}$) in Table 4 appear to lie on the extrapolation of the predicted curve of ζ_0 (for ω_0 = 1 and 0) as seen in Table 3 and Figure 3.

Regarding the other related tube parameters in Table 4, brief comments are made as follows. Apparently, for the ϕ_t values for the three different ϕ's, $\phi_t > \phi$ is satisfied, which is consistent with the unfrozen condition inside the tube. The D_M values at $\phi = 0.21$ and 0.48 in Table 4 are within the predicted range (for $\omega_0 = 1$ and 0) at the corresponding ϕ in Table 3. Also, N_{0t} is calculated using eq 9. In Tables 3 and 4, the N_{0t} value, which is the number of unfrozen diluent molecules in a tube, is estimated by assuming $\upsilon_m = 2.18$ nm^3 as van der Waals volume of the docosane molecule.[26] It is reasonable that the magnitude of N_{0t} determined for the three different ϕ's from the NMR data of ω_0 in Table 4 is less than the predicted maximum magnitude of N_{0t} (for $\omega_0 = 1$) for the corresponding mixtures in Table 3. The predicted values of N_{0t} (for $\omega_0 = 1$) for the mixtures are obviously smaller than those estimated for the NR−benzene mixtures at the corresponding concentration (see Table 2) and this is attributable to the fact that the molecular size of *n*-docosane is larger than that of benzene.

Temperature-Dependent Parameters. In the above analysis using the revised eq 6, we have used a temperature-independent value for several thermodynamic or physical parameters of the

mixtures despite different melting points, some of which must essentially change with temperature. Therefore, we examined to what extent the magnitude of crystal sizes for each mixture in Table 3 could vary when a different parameter value was used at the temperature around its melting point shown in the table. Of these parameters, particular attention is paid here to h_0, σ_0, V_0 (or d_0), and χ. First, we checked the heat of fusion of bulk *n*-docosane (h_0). That is, $h_0(T_m)$ values used for different ϕ's in Table 3 were all reduced by 5% of the original $h_0(T_m°)$ value, which should be an overeduction for *n*-docosane. However, the calculated crystal size increased only by less than 10% of their individual crystal sizes in Table 3 (although the recalculated results are not shown here). Apparently, this 10% variation is not too large in this calculation and thus the use of $h_0(T_m°)$ as a temperature-independent parameter does not cause an important problem in calculation even at different T_m.

When the influence of varying the σ_0 value was examined, recalculations of ζ_0 were done for the cases of the lower limit of $\sigma_0 = 8 \times 10^7$ J/cm^2 and the upper limit of $\sigma_0 = 1 \times 10^8$ J/cm^2 for the mixtures in Table 3. The lower limit value increased ζ_0 up to +15% of its initial value for $a = 0.81$ nm and decreased down to −20% for $a = 2.83$ nm, whereas the upper limit value decreased ζ_0 down to −15% for $a = 0.81$ nm and increased up to +20% for $a = 2.83$ nm. Namely, the use of the middle value of $\sigma_0 = 9 \times 10^7$ J/cm^2 results in calculation of ζ_0 within ±20% even in the case of $a = 2.83$ nm.

In addition to the density $d_0 = 0.779$ g/cm^3 at $T_m° = 44.1$ °C as used in the above calculation, Sayer et al.[31] gave a density (d_0) vs temperature (T) curve over 0−90 °C including its density change from the solid to the liquid phase at room temperature.[31,35] We could cite the density at T_m in Table 3 from the d_0 vs T curve, e.g., $d_0 \approx 0.777$ at $T = 44.5$ K for the $\phi = 0.21$ mixture and $d_0 \approx 0.905$ g/cm^3 at $T = 41.1$ K for the $\phi = 0.68$ mixture. For the other mixtures, we can remark only qualitatively that d_0 increases as T decreases within the d_0 range of 0.777−0.905 g/cm^3 over 41.1−44.5 °C. Recalculations of ζ_0 were carried out only for $\phi = 0.21$ and 0.68 using those density values. In consequence, the deviation of ζ_0 by the different d_0 values from the corresponding ζ_0 at $d_0 = 0.779$ becomes larger as ϕ is higher, but that deviation was up to approximately +20% at most for the $\phi = 0.68$ mixture. Hence, it may be said that the temperature independent and constant value of $d_0 = 0.779$ does not cause an important problem for all the mixtures in Table 3.

Finally, we comment on whether the use of $\chi = 0.30$ common to all the mixtures in this work is appropriate, which was previously determined by the mpd method of finding a best fit curve to the FH relation.[7] In the NR−benzene system we have already regarded χ as a function of temperature and concentration, as described in the earlier section, and this showed a more consistent concentration dependence of ζ_0 than that with the conventional fixed value $\chi = 0.43$, as reported in the previous paper.[8] On the other hand, to what extent does χ change with temperature and concentration in the IR−*n*-docosane system? We can expect that this change would be considerably small because even $\Delta T = 3.56$ °C for the $\phi = 0.68$ mixture in Table 3 is very small, compared with the level of $\Delta T \approx 18$ °C for the corresponding ϕ mixture of NR−benzene in Table 1. Furthermore, if the interaction parameter χ in the IR−*n*-docosane system was changed by ±7%, as similar to the variation of χ_M in NR−benzene (Table 1), the calculated ζ_0 deviates only +15% and −10%, respectively, from its original value at $\phi = 0.68$. Apparently, these deviations are not significantly large. Hence, we may conclude that to use $\chi = 0.30$, independently from temperature and concentration, does not cause an important problem in considering the results developed in the present IR−*n*-docosane systems.

Summary and Conclusions

In the present work, we proposed a revised model that attempts to account for the observed differences in the melting point depression of benzene in natural rubber mixtures and that of *n*-docosane in polyisoprene mixtures. The model is applicable to physical networks that are virtually formed only by entanglement couplings. In particular, the model considers an elastic term due to chain confinement by freezing, in addition to elastic terms from the Flory−Rehner model due to entanglement (FR[M_e]) effects.

The above elastic terms are added to the conventional Gibbs−Thomson equation for melting point depression due to size and to the Flory−Huggins expression, which predicts a melting point depression due to a mixing contribution to the free energy. We further have added a term of chain confinement based on a hard tube concept that is characterized by a frozen (straight) tube diameter (D_M) and a tube length (L) assuming that the crystal length (ζ_0) and the tube length are equal.

The results presented here can be summarized as follows: (1) The crystal shape depicted from estimated D_M and ζ_0 values is similar to that observed by electron microscopy.[17] (2) There is a ϕ dependence of ζ_0 in the un-cross-linked or lightly cross-linked mixtures, approaching the corresponding Flory's coil size in the higher range of ϕ.

It can be emphasized that, in the Flory affine model,[36,37] the mobility of cross-links forming a network is smaller than in the phantom model[38,39] in which the cross-links are considered to fluctuate greatly inside the network. Also, the Flory model involves the well-known logarithmic term due to a cross-link formation entropy that is volume dependent.[36,37] We think that our choice of the Flory model is justifiable because entanglements are greatly spatially confined by freezing and therefore the above volume dependent entropy effect would be needed as the result of entanglement coupling (similar to cross-linking) of the primary polymer chains. In the earlier work,[8] we found that the size evaluation by the Flory model was approximately 10−30% smaller than by the phantom model in the concentration range studied in the work,[8] which can be nearer to the corresponding Flory coil size. This additionally supports the Flory model, although not stated in the paper.[8] The results of the current modeling suggest that elastic effects due to chain swelling in the liquid state and chain confinement effects in the frozen state play a leading role in the melting point depression of solvents mixed with un-cross-linked mixtures.

Acknowledgment. Y.H. is grateful to Dr. G. B. McKenna of Texas Tech University for his helpful suggestions. He also thanks S&S Japan Co., Ltd. for partial support.

References and Notes

(1) Hildebrand, J. H.; Scott, R. L. *The Solubility of Nonelectrolytes*; Dover Publications: New York, 1964; Chapter 20.
(2) Orwall, R. A. *Rubber Chem. Technol.* **1977**, *50*, 451.
(3) Wittman, J. C.; Manley, R. St. J. *J. Polym. Sci. Polym. Phys. Ed.* **1977**, *15*, 1089.
(4) Zwiers, R. J. M.; Gogolewski, S.; Pennings, A. *J. Polymer* **1983**, *24*, 167.
(5) Dorset, D. L.; Hanlon, J.; Karet, G. *Macromolecules* **1989**, *22*, 2169.
(6) Jackson, C. L.; McKenna, G. B. *Rubber Chem. Technol.* **1991**, *64*, 760.
(7) Ikeda, Y.; Hoei, Y. *Chem. Express* **1992**, *6*, 425.
(8) Hoei, Y.; Ikeda, Y.; Sasaki, M. *J. Phys. Chem. B.* **1999**, *103*, 5353.

(9) Defay, R.; Prigogine, I.; Bellemans, A. *Surface Tension and Adsorption*; Longmans: London, 1966; Chapter 15.
(10) Boonstra, B. B.; Heckman, F. A.; Taylor, G. L. *J. Appl. Polym. Sci*. **1988**, *12*, 223.
(11) Arndt, K. F.; Zander, P. *Colloid Polym. Sci*. **1990**, *268*, 806.
(12) Oikawa, H.; Murakami, K. *J. Macromol. Sci. Phys*. **1989**, *B28*, 187.
(13) Hoei, Y.; Yamaura, K.; Matsuzawa, S. *J. Phys. Chem.* **1992**, *96*, 10584.
(14) Flory, P. J. *Principle of Polymer Chemistry*; Cornell University Press: Ithaca, NY, 1953; Chapter 13. Flory, P. J.; Rehner, J., Jr. *J. Chem. Phys*. **1943**, *11*, 521.
(15) Frenkel, J. *Rubber Chem. Technol*. **1940**, *13*, 264
(16) (a) Graessley, W. W. *Physical Properties of Polymers*; American Chemical Society: Washington, DC, 1993; Chapter 3. Graessley, W. W. *Adv. Polym. Sci*. **1982**, *47*, 67. (b) Ferry, J. D. *Viscoelastic Properties of Polymers*; John Wiley and Sons: New York, 1980; Chapters 10−14 and 17. (c) Nemoto, N.; Moriwaki, M.; Odani, H.; Kurata, M. *Macromolecules* **1971**, *4*, 215.
(17) Kanig, G.; Karge, H. *J. Colloid Interface Sci*. **1966**, *21*, 649.
(18) de Gennes, P. G. *Scaling Concept in Polymer Physics*; Cornell University Press: Ithaca, NY, 1979; Chapter 1 and 3.
(19) Fetters, L. J.; Lohse, D. J.; Richter, D.; Witten, T. A.; Zirkel, A. *Macromolecules* **1994**, *27*, 4640. Fetters, L. J.; Lohse, D. J.; Colby, R. H. *Physical Properties of Polymers Handbook*; AIP Press: New York, 1996; Chapter 24.
(20) He, T.; Porter, R. S. *Macromol. Chem., Theory Simul*. **1992**, *1*, 119.
(21) Zang Y−H.; Carrenau, P. J. *J. Appl. Polym. Sci*. **1991**, *42*, 1965.
(22) Privalko, V. P.; Lipatov, Y. S. *Macromol. Chem*. **1974**, *175*, 641.
(23) Daud, M.; de Gennes, P. G. *J. Phys. (Paris)* **1977**, *38*, 85.
(24) Jackson, C. L.; McKenna, G. B. *J. Chem. Phys.* **1990**, *93*, 9002.
(25) Kitaigorodsky, A. I. *Molecular Crystals and Molecules*; Academic Press: New York and London, 1973; p 18. Kitaigorodsky, A. I. *Mixed Crystals*; Solid-State Science 33; Springer-Verlag: Berlin, Heidelberg, New York, Tokyo, 1984; p 71.
(26) The benzene molecules volume was estimated at 0.15 nm^3 from the liquid density (∼0.9 g/cm^3) or from the known volume increments of an aromatic carbon atom and the carbon−hydrogen bond in ref 25.
(27) Maron, S. H.; Nakajima, N.; Krieger, I. M. *J. Polym. Sci*. **1959**, *37*, 1. Maron, S. H.; Nakajima, N. *J. Polym. Sci*. **1960**, *42*, 327. Maron, S. H.; Nakajima, N. *J. Polym. Sci*. **1960**, *42*, 327.
(28) Suga, H., Ed. *Kagaku Binran II*, 3rd ed.; Japan Chem. Soc., Maruzen: Tokyo, 1984; p II-252.
(29) A sample of a commercial product Kuraprene IR-10 manufactured by Kuraray Co., Ltd. was used after being dissolved in benzene and then reprecipitated from methanol. The gel-permeation-chromatography average molecular weight after extraction with benzene is approximately 8×10^5.
(30) Turnbull, D.; Cormia, R. L. *J. Chem. Phys*. **1961**, *34*, 820.
(31) Sayer, WM. F.; Patterson, R. F.; Keays, J. L. *J. Am. Chem. Soc*. **1943**, *66*, 179.
(32) Fusegawa, K., Ed. *Wax no Seishitsu to Oyo*; Saiwai-shoboh; Tokyo, 1985; p 63.
(33) Rigaku Denki Bunseki Center, *X-sen Kaiseki no Tebiki*, 4th ed.; Rigaku Denki, Ed.; Sanseido: Tokyo, 1989; p 91.
(34) Hoei, Y.; Moteki, Y.; Shackleton, J. S. *J. Polym. Sci., Part B, Polym. Phys*. **1998**, *36*, 1293.
(35) Templin, P. R. *Ind. Eng. Chem*. **1956**, *48*, 154.
(36) Flory, P. J. *Principle of Polymer Chemistry*; Cornell University Press: Ithaca, NY, 1953; Chapter 11.
(37) Hill, T. L. *An Introduction to Statistical Thermodynamics*; Addison-Wesley Publishing Co. Inc.: Reading, MA, 1960; Chapter 21.
(38) Mark, J. E.; Erman, B. *Rubber Elasticity A Molecular Primer*; John Wiley & Sons: New York, 1988; Chapter 29.
(39) James, H. M. *J. Chem. Phys*. **1947**, *15*, 651. James, H. M.; Guth, E. *J. Chem. Phys*. **1947**, *15*, 669. James, H. M.; Guth, E. *J. Chem. Phys*. **1953**, *21*, 1039.